

SIMULATION OF THE ESS PROTON BEAM WINDOW SCATTERING

E. Fackelman, K. Sjobak*, H. Gjersdal, E. Adli, University of Oslo, Oslo, Norway
 C. Thomas, Y. Levinsen, A. Takibayev, European Spallation Source, Lund, Sweden

Abstract

The European Spallation Source produces neutrons used for science by delivering a 5 MW proton beam to a tungsten target. The proton beam parameters must remain within a well-defined range during all phases of facility exploitation. The proton beam parameters are measured and monitored by an instrumentation suite, among which are two beam imaging systems. Parameters such as position and beam current density can be calculated from the images, supporting beam tuning and operation. However, one of the two systems may be affected by beam scattering. In this paper, we will focus on modelling the impact of the scattering on the beam on target distribution. The modelling process, involving simulation codes such as Geant4 and two-dimensional convolution in Matlab, is described. Initially, Geant4 simulates a scattered pencil beam. The resulting distribution is fitted and can be used similarly to an instrument response in image processing to model any possible beam distribution. Finally, we discuss the results of the scattered beam imaging model, showing the range of applications of the model and the impact of scattering on the beam parameters.

BACKGROUND

Before hitting the tungsten target of the European Spallation Source (ESS), the beam passes through the Proton Beam Window (PBW), which separates the accelerator vacuum from the target vacuum, as illustrated in Fig. 1. This passage through matter scatters the beam, increasing the footprint size on the front surface of the target. The footprint of each bunch is already enlarged using magnetic quadrupoles, and each bunch is placed at different locations on the target by fast rastering kicker magnets [1]. If the footprint is smaller than expected due to, e. g. a magnet failure, it can damage the target and the PBW. Furthermore, if the beam is larger than expected, it can damage equipment surrounding the target and beamline components. For this reason, the Target Imaging System (TIS) continuously produces images of the beam at the target and the PBW, which are coated with a luminescent material. The TIS will help the operators, and eventually automatic systems, detect and react to errant beam conditions before they damage the target region. However, the particle distribution during nominal beam conditions must be known for this to work well. Describing this distribution is part of the goal of the work described in this paper, which will also help in understanding abnormal scenarios.

* k.n.sjobak@fys.uio.no

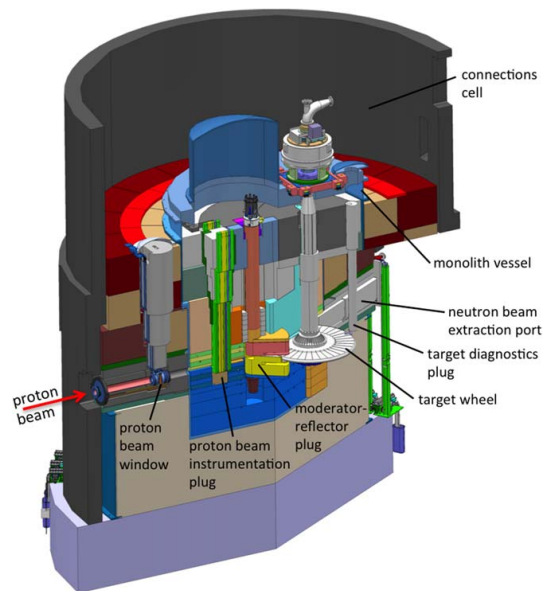


Figure 1: Illustration of the layout of the ESS target region. The beam comes in from the left, passing through the PBW and through the aperture of the proton beam instrumentation plug and also between the “wings” of the neutron moderator/reflector, before hitting the target wheel. Image from Ref. [2].

SETUP

Simulation with Geant4/MiniScatter

The main simulation tool used in this work is MiniScatter [3]. This is an application built on Geant4 [4–6] with a Python wrapping which makes it easy to create or load particle distributions, setup simple geometries, and extract information in the form of ROOT [7] histograms and trees. For this simulation, the QGSP_BERT_EMZ physics list was used with a production cut of 100 μm .

Geant4 handles the tracking of particles through the experiment, until they either exit the simulation volume or lose all their energy. For each step a particle makes, the energy loss, scattering angle, and whether to do secondary particle generation is decided via the Monte Carlo method, taking the particle and material properties into account.

The Proton Beam Window was modelled as shown in Fig. 2 (a), with a 1.25 mm thick front surface made from aluminum, a 2 mm water cooling channel, and a 1 mm back surface of aluminum. The radius of curvature of the downstream surface is 88 mm, and the horizontal/vertical size is 200 \times 160 mm^2 . The model is based on the design model [8, 9].

The overall geometry used for the MiniScatter simulation is shown in Fig. 2 (b), indicating the plane where the particles

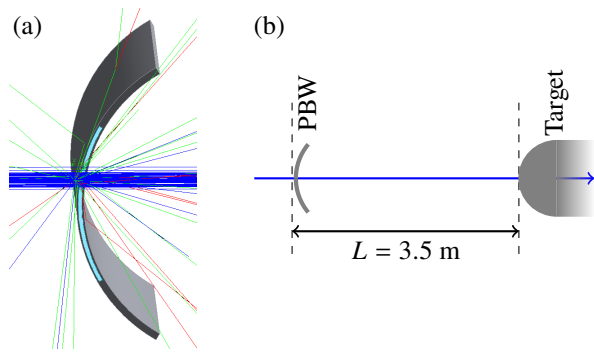


Figure 2: (a) Proton Beam Window (PBW) model in MiniScatter, with a few initial particle trajectories. (b) Relative position of elements for simulation.

are loaded in front of the PBW and where they are scored in front of the target. Note that this simulation did not include the whole geometry of the target area, including the shielding blocks, the plugs and the instrumentation.

In the results presented in this paper, a pencil beam was used, with all the particles having the same initial position $x = y = 0$ and angle relative to the beamline axis $x' = y' = 0$. All the initial particles are protons, and have an energy of 570 MeV.

The main observable extracted from the simulation is the $\{x, y\}$ distribution of protons with $E_k > 564$ MeV, which was put into 2D histograms for analysis. An example of such a histogram is shown in Fig. 3.

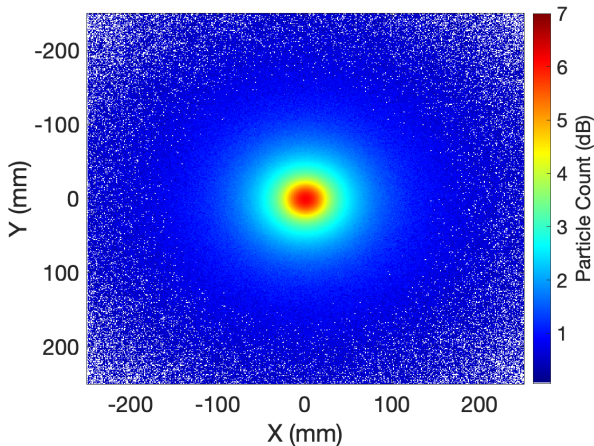


Figure 3: Geant4 particle distribution of the scattered pencil beam on the target surface, with 4.9×10^8 particles.

Rastering of the Beam

The beam delivery system contains a set of fast dipole magnets that deflect the beam in both horizontal and vertical planes. The deflection in each plane is periodic, following a triangular saw-tooth pattern asynchronous to each other so that the beam distributes over a rectangular shape. The expected raster-scan profile can be described using the function

$$\text{erf}(z) \equiv \frac{2}{\sqrt{\pi}} \int_{-\infty}^z \exp(-t^2) dt \text{ function in Eq. (1)}$$

$$P(x, y) = 0.5 \cdot \left[\text{erf} \left(\frac{x + a_x - C_x}{\sqrt{2}\sigma_x} \right) - \text{erf} \left(\frac{x - a_x - C_x}{\sqrt{2}\sigma_x} \right) \right] \dots \\ \cdot 0.5 \cdot \left[\text{erf} \left(\frac{y + a_y - C_y}{\sqrt{2}\sigma_y} \right) - \text{erf} \left(\frac{y - a_y - C_y}{\sqrt{2}\sigma_y} \right) \right], \quad (1)$$

where $a_{x,y}$ is the raster amplitude, $C_{x,y}$ the beam offset, and $\sigma_{x,y}$ the rms beam size at the PBW [10]. The rastered beam particle distribution was initialized 2 mm before the PBW within MiniScatter and tracked during the scattering within the PBW and the drift to the target surface. The nominal beam distribution at the target from rastering and scattering is shown in Fig. 4. The rastered beam is simulated in MiniScatter separately from the single bunch and pencil beam.

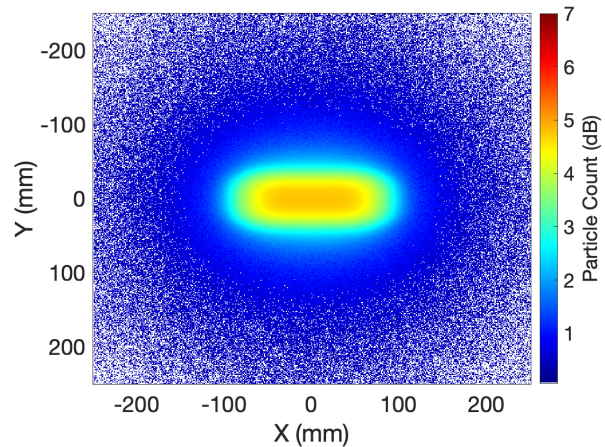


Figure 4: Geant4 raster beam distribution, with 2.8×10^8 particles.

RESULTS

Fit of the Scattered Pencil Beam

In order to enable rapid evaluation of the effect of scattering when changing the initial beam parameters without going through the full Geant4 simulation, it is desired to have an analytical description of how the PBW modifies the beam distribution. For this, a static pencil beam is simulated passing through the PBW with Geant4, and the profile of the density (Fig. 3) is taken around $|x| < 250$ mm, i. e. 4 degrees scattering angle. It is then fitted to a sum of N Gaussian functions as described by Eq. (2), and shown in Fig. 5, where A_i are the weights, (x_c, y_c) the centre, and σ_i the rms value of the i -th 2D-Gaussian, and $r = (x - x_c)^2 + (y - y_c)^2$;

$$P(x, y) = \sum_{i=1}^N \frac{A_i}{2\pi\sigma_i} \exp \left(\frac{-r^2}{2\sigma_i^2} \right). \quad (2)$$

The motivation for the sum is to fit the tails of the distribution. While multiple Coulomb scattering can well

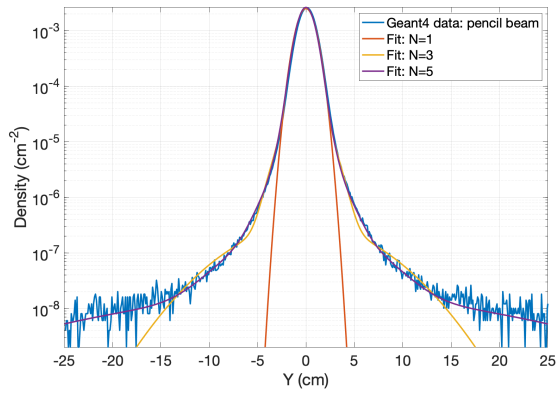


Figure 5: Fitting of scattered pencil beam distribution with sum of N 2D-Gaussians.

be described with a single Gaussian distribution, it does not capture the tails of the distribution. The fit is done in Python, using the Nelder-Mead Simplex algorithm from the `scipy.optimize.minimize` package [11].

The resulting fit parameters are listed in Table 1. The fit function used fits with $2 \times N$ parameters, where N is the number of Gaussians summed, returning N weights and N rms values. The fit of the scattered pencil beam has been done with increasing N , and reporting the χ^2 test result. A correct model leads to χ^2 converging to $(\nu - 2N)$, where ν is the number of tests, i. e. the size of the image in this case (500×500 pixels). From Table 1, one can read that χ^2 converges to this value. For $N = 5$, $\frac{\chi^2}{\nu - 2N} \approx 1.09$. Hence, $N = 5$ provides a satisfactory result, fitting the wings with sufficient accuracy. $N > 5$ provides lower χ^2 tests, but with marginal improvement and higher computational cost. A plot of the scattered pencil profile and the resulting fit functions with N up to 5, Fig. 5, illustrates the result of the fit.

Table 1: Weight (A) and σ for sums of N Gaussians to fit the beam density from Fig. 5, $\chi_{\text{ref}}^2 = \nu - 2N$

N	1	2	3	4	5	6
σ_1 [mm]	7.32	7.34	7.39	7.47	7.58	7.34
σ_2 [mm]		18.2	15.7	13.2	10.7	10.7
σ_3 [mm]			55.0	31.1	21.9	17.7
σ_4 [mm]				130.0	46.9	31.9
σ_5 [mm]					166.0	65.0
σ_6 [mm]						201.0
A_1 [1×10^{-1}]	1	9.43	9.21	8.85	8.48	8.21
A_2 [1×10^{-2}]		5.69	7.33	9.94	12.4	13.8
A_3 [1×10^{-3}]			6.04	12.1	20.5	29.3
A_4 [1×10^{-3}]				3.09	4.25	7.47
A_5 [1×10^{-3}]					2.83	2.07
A_6 [1×10^{-3}]						2.82
χ^2 [1×10^5]	118.9	27.61	10.93	3.466	2.729	2.661
$\chi^2/\chi_{\text{ref}}^2$	47.5	11.0	4.37	1.38	1.09	1.06

Convolution with Rastered Beam Distribution

In order to compare the scattered pencil beam with the Geant4 scattered rastered beam (Fig. 4), the fit Gaussian

sums are convolved with the reference raster equation, Eq. (1) in Fig. 6, showing the vertical slice around $|x| < 250$ mm. The Gaussian fits from $N = 1$ to $N = 6$ are included in Fig. 6 to show the difference the extra Gaussians makes in matching the tails. The 5-Gaussians fit convolved with the reference raster profile matches well with the raster slice up until ± 200 mm or ± 3.6 degrees.

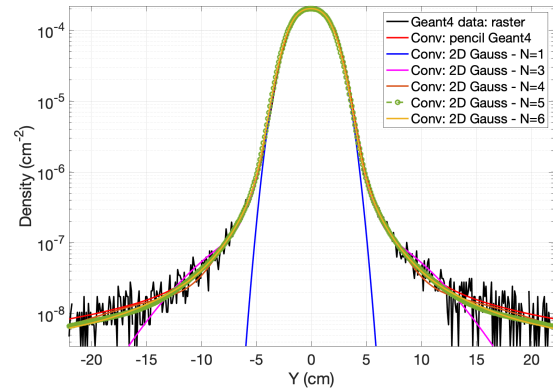


Figure 6: Profiles of 2D scattered rastered beam distributions compared to convolution of pencil beams or fit pencil beams with Eq. (1).

CONCLUDING REMARKS

The method applied to model the PBW scattering seems consistent with the full Geant4 simulation. It can predict with moderate accuracy how any beam current distribution can distort after the PBW scattering. It is sufficient for modelling the images from the TIS and, in first approximation, to understand what impact the scattering has on the beam properties measurement. In return, it can be applied to understand the TIS performance and how it can support beam tuning and operation. For the specific condition studied, the scattered pencil beam rms value is expected to be larger than 8 mm. The resulting rms value is expected to vary for other ESS beam energies. However, the net effect of the scattering is to prevent a tight-focused beam on the target, which can be seen as a protective effect. Predicting the scattered distribution for various input distributions provides the initial condition for thermo-mechanical studies of the target area components. Our approach permits faster modelling of the target beamline components' temperature and stress, exploring a considerable space of beam parameters, which would be time-consuming if all possible distributions were modelled using codes such as Geant4 or MCNPX [12]. At this stage, further investigation of the model is still required. Modelling the scattered pencil beam for a range of energies and various PBW thicknesses should help refine the method in view of the commissioning of the first beam on target.

REFERENCES

- [1] H. D. Thomsen and S. P. Møller, "The Beam Delivery System of the European Spallation Source," in *Proc. HB'16*, Malmö,

- Sweden, Jul. 2016, pp. 427–432.
doi:10.18429/JACoW-HB2016-WEAM7Y01
- [2] R. Garoby *et al.*, “The European Spallation Source Design,” *Phys. Scr.*, vol. 93, no. 1, p. 014 001, 2017.
doi:10.1088/1402-4896/aa9bfff
- [3] K. Sjobak and H. Holmestad, “MiniScatter, a Simple Geant4 Wrapper,” in *Proc. IPAC’19*, Melbourne, Australia, May 2019, pp. 3152–3155.
doi:10.18429/JACoW-IPAC2019-WEPTS025
- [4] S. Agostinelli *et al.*, “Geant4 – a simulation toolkit,” *Nucl. Instrum. Methods Phys. Res., Sect. A*, vol. 506, no. 3, pp. 250–303, 2003. doi:10.1016/S0168-9002(03)01368-8
- [5] J. Allison *et al.*, “Geant4 developments and applications,” *IEEE Trans. Nucl. Sci.*, vol. 53, no. 1, pp. 270–278, 2006.
doi:10.1109/TNS.2006.869826
- [6] J. Allison *et al.*, “Recent developments in geant4,” *Nucl. Instrum. Methods Phys. Res., Sect. A*, vol. 835, pp. 186–225, 2016. doi:10.1016/j.nima.2016.06.125
- [7] R. Brun and F. Rademakers, “Root – an object oriented data analysis framework,” *Nucl. Instrum. Methods Phys. Res., Sect. A*, vol. 389, no. 1, pp. 81–86, 1997.
doi:10.1016/S0168-9002(97)00048-X
- [8] PBW Assembly ESS-3805683, ESS, Lund, Sweden, 2021.
- [9] R. Vivanco *et al.*, “ESS Proton Beam Window Design Update,” *J. Phys. G: Nucl. Part. Phys.*, vol. 1021, p. 012 065, 2018. doi:10.1088/1742-6596/1021/1/012065
- [10] R. Miyamoto and H. Thomsen, “Parametric Study of the Beam Footprint Characteristics on the ESS Target,” in *Proc. IPAC’18*, Vancouver, BC, Canada, Apr.-May 2018, pp. 866–869. doi:10.18429/JACoW-IPAC2018-TUPAF062
- [11] P. Virtanen *et al.*, “SciPy 1.0: Fundamental Algorithms for Scientific Computing in Python,” *Nat. Methods*, vol. 17, pp. 261–272, 2020. doi:10.1038/s41592-019-0686-2
- [12] The MCNP® Code. <https://mcnp.lanl.gov>